

# Design, Synthesis, Antibacterial Activity, and Mechanisms of Novel 1,3,4-Thiadiazole Derivatives Containing an Amide Moiety

Zhibing Wu, Jin Shi, Jixiang Chen, Deyu Hu,\* and Baoan Song\*



Cite This: <https://doi.org/10.1021/acs.jafc.1c01626>



Read Online

ACCESS |



Metrics & More



Article Recommendations



Supporting Information

**ABSTRACT:** To discover novel antibacterial agents, a series of novel 1,3,4-thiadiazole derivatives containing an amide moiety were designed and synthesized, and their antibacterial activities were tested. Compound **30** was designed and synthesized according to the CoMFA model. Compound **30** exhibited higher antibacterial activities against *Xanthomonas oryzae* pv. *oryzicola* and *Xanthomonas oryzae* pv. *oryzae*, with EC<sub>50</sub> values of 2.1 and 1.8 mg/L, respectively, which were superior to those of thiodiazole copper (99.6 and 92.5 mg/L). The protective and curative activities of compound **30** against rice bacterial leaf blight were 51.3 and 46.1%, respectively, which were better than those of thiodiazole copper (37.8 and 38.5%). The protective and curative activities of compound **30** against rice bacterial leaf streak were 45.9 and 40.5%, respectively, which were better than those of thiodiazole copper (36.2 and 31.1%). In addition, the protective activity of compound **30** against rice bacterial leaf streak was related to increased activities of related defense enzymes and upregulated the differentially expressed proteins of the glycolysis/gluconeogenesis pathway.

**KEYWORDS:** 1,3,4-thiadiazole derivatives, defense enzymes, mechanism of action, CoMFA

## INTRODUCTION

Bacterial leaf blight (BLB) and bacterial leaf streak (BLS), caused by *Xanthomonas oryzae* pv. *oryzae* (*Xoo*) and *Xanthomonas oryzae* pv. *oryzicola* (*Xoc*), respectively, not only are the two main rice bacterial diseases but also represent unsolved problems, which seriously threaten the safety of rice production and cause reductions in rice yield of 20–50%,<sup>1,2</sup> particularly in humid tropical and subtropical areas of Asia and Africa.<sup>3–5</sup> At present, the management of rice bacterial diseases mainly relies on traditional chemical antibacterial agents, such as bismethiazol, streptomycin, and thiodiazole copper.<sup>6,7</sup> However, the long-term use of these traditional antibacterial agents and the deterioration of the environment have led to poor control of rice bacterial diseases.<sup>8,9</sup> Therefore, the identification of novel antibacterial agents is still a huge challenge in the management of rice bacterial diseases.

The 1,3,4-thiadiazole ring is easily attacked by nucleophiles and reacts to produce various derivatives.<sup>10</sup> The 1,3,4-thiadiazole derivatives have a wide range of biological activities, such as antibacterial,<sup>11–13</sup> antifungal,<sup>14,15</sup> insecticidal,<sup>16,17</sup> antiviral,<sup>18</sup> and antitumor<sup>19</sup> activities, and play an important role in drug discovery, especially in the discovery of antibacterial agents against rice bacterial diseases. A series of 1,3,4-thiadiazole derivatives were synthesized and some compounds revealed good bioactivities against *Xoo*, *Xanthomonas axonopodis* pv. *citri*, and *Xoc*<sup>8,11–13</sup> in our previous works. Amide derivatives play an important role in drug discovery and exhibit diverse biological activities, such as insecticidal,<sup>20–22</sup> antibacterial,<sup>23–25</sup> anti-inflammatory,<sup>26</sup> antiviral,<sup>27,28</sup> and anticancer activities.<sup>29</sup> To date, many amide compounds have been successfully developed for use as fungicides, such as fluopimomide, boscalid, and orysastrobin, but commercial antibacterial agents do not have amide compounds.

To discover new antibacterial agents with high antibacterial activity, an amide structure was introduced into the skeleton of 1,3,4-thiadiazole to design and synthesize a series of novel 1,3,4-thiadiazole derivatives containing an amide moiety, and their antibacterial activity was systematically evaluated. In addition, a CoMFA model was constructed based on the EC<sub>50</sub> values of compounds **1–29** against *Xoc*. Compound **30** was designed and synthesized according to the CoMFA model (Figure 1). The antibacterial activities of compound **30** against *Xoc* and *Xoo* were evaluated. Additionally, the antibacterial action mechanism of compound **30** was investigated through related defensive enzyme activities and proteomics research.

## MATERIALS AND METHODS

**Chemicals and Instruments.** All raw materials and solvents required for the reactions were provided by Guiyang Yuda Chemical Co., Ltd., China. The NMR spectra of all compounds were collected on a DPX Ascend-400 spectrometer (Bruker, Germany) with a JMTC-500/54/JJ Superconducting Magnet (JEOL, Tokyo, Japan). HRMS spectra of compounds were collected with Thermo Scientific Q Exactive (Thermo, USA). The morphology of pathogenic bacteria was observed using Nova-Nano-SEM-450 (FEI, USA).

**Preparation of Target Compounds 1–4.** Anthranilic acid (2.0 mmol) and formamide (8.0 mmol) were refluxed at 150–160 °C for 3–4 h. After the reaction was completed, the system temperature was decreased to 100 °C, and the reaction was transferred to a beaker and supplemented with an appropriate amount of water. Intermediate **A** was

Received: March 19, 2021

Revised: June 20, 2021

Accepted: July 9, 2021

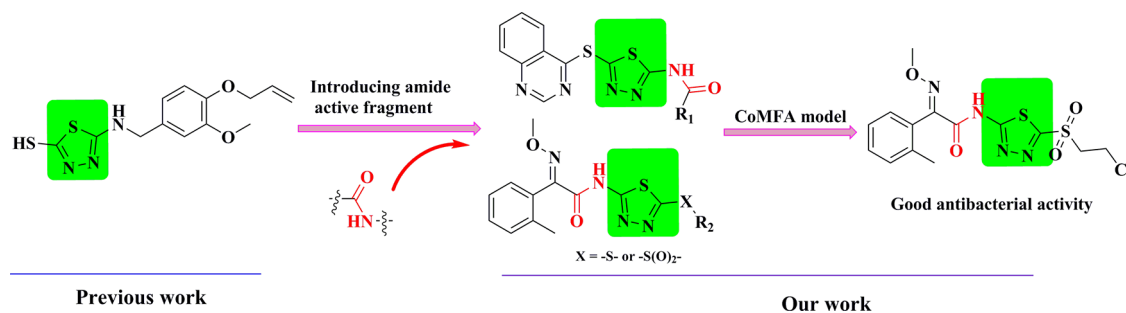


Figure 1. Design of the target compounds.

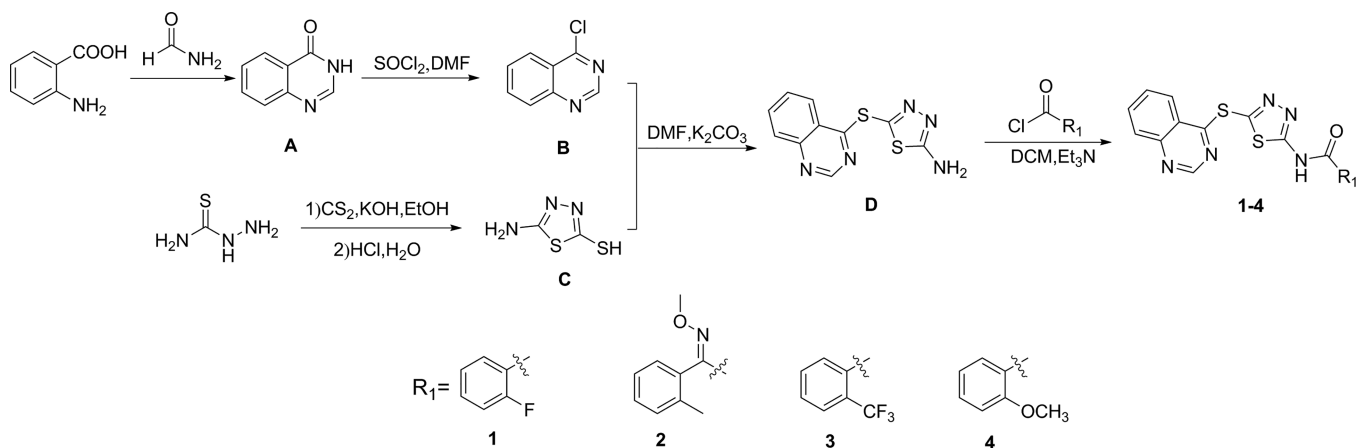


Figure 2. Synthetic route of compounds 1–4.

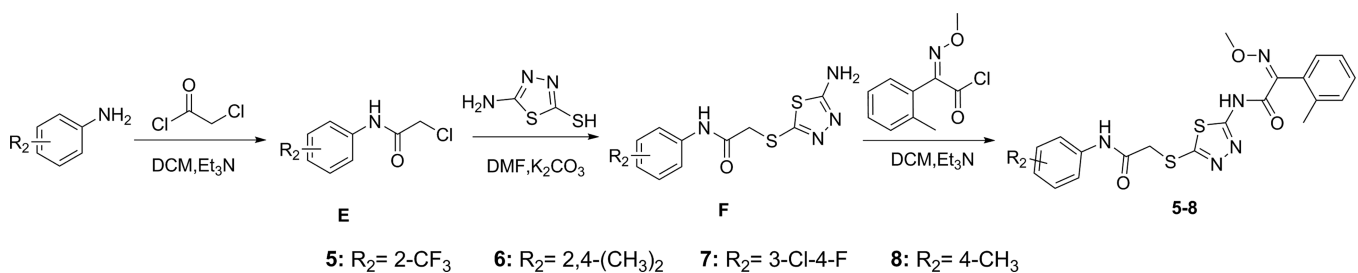


Figure 3. Synthetic route of compounds 5–8.

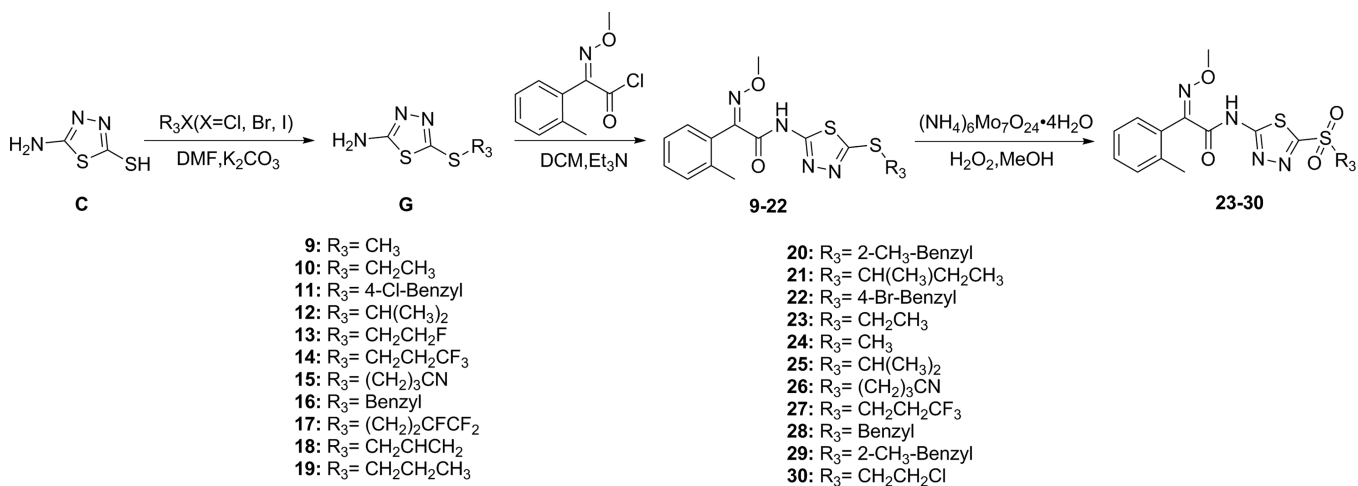


Figure 4. Synthetic route of compounds 9–30.

obtained by recrystallization.<sup>30</sup> Intermediate A (13.7 mmol) was dissolved in 1,2-dichloroethane (DCM), and then thionyl chloride (20

mL) and *N,N*-dimethylformamide (1 mL, DMF) were added to a refluxed reaction flask for 4–5 h. After the reaction was completed,

DCM was extracted and recrystallized with petroleum ether to obtain intermediate **B**. Thiosemicarbazide (32.9 mmol), potassium hydroxide (49.4 mmol), and carbon disulfide (49.4 mmol) were added to absolute ethanol (60 mL) and reacted for 8–10 h. After the reaction was completed, the reaction system was stirred in water and adjusted to acidity with dilute hydrochloric acid. Intermediate **C** was collected by suction filtration.<sup>31</sup> Intermediate **C** (4.6 mmol) and potassium carbonate (6.9 mmol) were stirred in DMF (2 mL) for 20 min. Next, intermediate **B** (4.6 mmol) was added to the reaction system and reacted for 2–6 h. Then, the reaction system was poured into water and stirred until solid precipitation to obtain intermediate **D**. Intermediate **D** (2.6 mmol) and triethylamine (3.8 mmol) were dissolved in DCM (20 mL), and the differently substituted benzoyl chlorides (2.6 mmol) were dropped slowly into the reaction flask and reacted for 1–6 h. Finally, target compounds 1–4 were obtained by column chromatography (Figure 2).

**Preparation of Target Compounds 5–8.** Differently substituted aniline (2.6 mmol) and triethylamine (3.8 mmol) were dissolved in DCM (20 mL), and chloroacetyl chloride (2.6 mmol) was dripped slowly into the reaction flask and reacted for 2–6 h (Figure 3). Then, intermediate **E** was obtained by extraction with DCM and recrystallization with petroleum ether. Intermediate **C** (4.6 mmol) and potassium carbonate (6.9 mmol) were stirred in DMF (2 mL), and intermediate **E** (4.6 mmol) was added to the reaction system and reacted for 2–6 h. After the reaction was completed, an appropriate amount of water was added to wash the product, and then intermediate **F** was obtained by filtration and recrystallization. (*E*)-2-(Methoxyimino)-2-(*o*-tolyl)acetyl (2.6 mmol) was dropped slowly into the DCM mixture of intermediate **F** (2.6 mmol) and triethylamine (3.8 mmol) to react for 1–6 h. Finally, crude target compounds 5–8 were obtained by column chromatography.

**Preparation of Target Compounds 9–30.** Intermediate **C** (4.6 mmol) and potassium carbonate (6.9 mmol) were added to DMF (2 mL). Then, different halogenated hydrocarbons or benzyl chloride (4.6 mmol) was added to the above system, and the reaction was completed after 2–6 h (Figure 4). An appropriate amount of water was added for washing, and intermediate **G** was obtained by filtration. (*E*)-2-(Methoxyimino)-2-(*o*-tolyl)acetyl chloride (2.6 mmol) was dropped slowly into the DCM mixture of intermediate **G** (2.6 mmol) and triethylamine (3.8 mmol). The reaction was completed after 1–6 h, and the target compounds 9–22 were obtained by column chromatography. Compounds 9–22 were oxidized in an ethanol mixture of 30% hydrogen peroxide (8.0 mmol) and ammonium molybdate (0.15 mmol) for 3–6 h under ice bath conditions. Finally, target compounds 23–30 were obtained by column chromatography.

**Antibacterial Activity *In Vitro* Assay.** The antibacterial activities *in vitro* of compounds 1–30 were tested by the turbidimetric method.<sup>32,33</sup> Thiodiazole copper was used as a positive control, and a test solution containing no compound was used as a negative control. All target compounds were dissolved in DMSO, diluted to the required concentration with 0.1% Tween-20, and then added to a test tube containing nutrient solution (NB) medium. Then, the test tube was incubated with shaking for 24–36 h at 180 rpm and 28 °C, and the absorbance (OD<sub>595</sub>) was measured at 595 nm. The test was repeated three times, with three parallel tests each time.

**3D-QSAR Analysis.** The CoMFA model was established on the Cloud 3D-QSAR server (<http://chemistry.cnu.edu.cn/cdb/server/cloud3dQSAR/>).<sup>34</sup> The SMILES format of all compounds was submitted. Twenty-one compounds were selected as the training set, and eight compounds were used as the test set. The pEC<sub>50</sub> values of all compounds were uploaded to the server. Compound 2 was used as a the template molecule. The partial least squares (PLS) regression approach was used to perform CoMFA analysis. The cross-validation coefficient ( $q^2$ ), non-cross-validation coefficient ( $r^2$ ), and corresponding non-cross-validation coefficient of the prediction ( $r^2_{\text{pred}}$ ) were used to evaluate the CoMFA model. Predicted pEC<sub>50</sub> values, steric field, and electrostatic field models were obtained from the Cloud 3D-QSAR server. The PyMol software (version 2.1) was used to visualize steric and electrostatic field models.

**Antibacterial Activity *In Vivo* Assay.** The antibacterial activity *in vivo* of compound 30 against BLB was evaluated.<sup>35,36</sup> Compound 30 and a positive control were diluted into a test solution of 200 mg/L. Thiodiazole copper was used as a positive control, and the same concentration of the solution without the compound was used as a negative control. The curative activity was tested according to the following steps. The rice leaves of “fengyouxiangzhan” at the six- to eight-leaf stage were inoculated with *Xoo* by the leaf-cutting method, and the test solution was sprayed evenly on the rice leaves 24 h after inoculation. The protective activity was tested similarly. After the test solution was sprayed on rice leaves for 24 h, *Xoo* was inoculated on the rice leaves. After 14 days of cultivation in the greenhouse, the lengths of rice leaf lesions were measured, and the antibacterial activity of compound 30 was calculated and analyzed using the disease index. The test was repeated three times.

The antibacterial activity *in vivo* against BLS was evaluated using previously reported methods.<sup>37</sup> The curative activity was tested according to the following steps. The rice leaves at the six- to eight-leaf stage were inoculated with *Xoc* by the pressure penetration method. When inoculating, the back of the leaf was facing up, 1 mL of the *Xoc* solution was aspirated with a sterile syringe without a needle, and then the bacterial solution was gently pressed into the leaves. After 24 h, the test solution was sprayed onto the rice leaves, and the protective activity was tested. After the test solution was sprayed on the rice leaves for 24 h, *Xoc* was inoculated on the rice leaves. After 14 days of cultivation in the greenhouse, the length of rice leaf lesions was measured, and the equation below was used to calculate the antibacterial activity of compound 30 against BLS. The test was repeated three times. In the following equation, *C* and *T* mean the length of the rice leaf lesion for the negative control and treatment groups, respectively.

$$\text{Antibacterial activity } I(\%) = (C - T) / C \times 100$$

**Morphological Changes.** According to previously reported methods,<sup>38,39</sup> the changes in the cell surface morphology after compound 30 treatment were observed using SEM. The *Xoo* or *Xoc* solution was washed three times and suspended in 1 mL of phosphate-buffered saline (PBS). Next, the DMSO solution containing compound 30 was diluted to 200, 50, 25, and 5 mg/L using PBS and incubated at 28 °C for 10 h. The test solution lacking the compound was used as a negative control. Cells were fixed with 2.5% glutaraldehyde for 8 h, and then anhydrous ethanol with different concentration gradients was used for dehydration. Finally, all the samples were observed after freeze-drying and coating with gold.

**Defensive Enzyme Activity.** The changes in the contents of the defensive enzymes (phenylalanine ammonia lyase (PAL), catalase (CAT), superoxide dismutase (SOD), and peroxidase (POD)) were calculated in rice leaves 1, 3, 5, and 7 days after rice infection with *Xoc* under greenhouse conditions using relevant enzyme kits (Suzhou Keming Biotechnology Co., Ltd.) for testing.

**Differentially Expressed Protein Analysis.** **Preparation of Rice Samples.** Compound 30 was diluted into a test solution (200 mg/L) to spray on rice leaves at the six- to eight-leaf stage. After the test solution was sprayed for 24 h, rice were inoculated with *Xoc*. The negative control was treated in the same way. Then, the rice samples were quick-frozen and ground.

**Total Protein Extraction and Identification.** The extraction and identification of total rice protein were carried out according to our previous works.<sup>40,41</sup>

**Bioinformatics Analysis.** The differentially expressed proteins (DEPs) were analyzed and classified by Gene Ontology (GO) annotations on the Kyoto Encyclopedia of Genes and Genomes (KEGG) and Uniprot software. GO annotations can be divided into three categories including cellular components, biological processes, and molecular functions. Additionally, KEGG annotations were retrieved from the KEGG database (<https://www.genome.jp/kegg/pathway.html>). For target lists with unlabeled proteomics results, the GO database was downloaded as a backend list. The tags corresponding to DEPs with differential expression levels >1.5 were marked in the GO database, and the protein content of each GO term was calculated.

## RESULTS AND DISCUSSION

**Chemistry.** Compounds 1–30 were synthesized according to the synthetic route. Anthranilic acid as the raw material and target compounds 1–4 were obtained through cyclization, chlorination, and substitution reactions. Target compounds 5–8 and 9–22 were obtained by the substitution reactions of intermediate F and intermediate G with (*E*)-2-(methoxyimino)-2-(*o*-tolyl)acetyl chloride, respectively. Subsequently, target compounds 23–30 were obtained by oxidation reactions. The physical and chemical properties and the <sup>1</sup>H NMR, <sup>13</sup>C NMR, and HRMS spectra of all target compounds are presented in Supporting Information I.

**Antibacterial Activities *In Vitro*.** As summarized in Table 1, some compounds exhibited good *in vitro* activities against *Xoo*

**Table 1. Antibacterial Activities *In Vitro* of Target Compounds 1–30 against *Xoo* and *Xoc*<sup>a</sup>**

compounds	<i>Xoo</i>		<i>Xoc</i>	
	50 mg/L (%)	EC <sub>50</sub> (mg/L) <sup>b</sup>	50 mg/L (%)	EC <sub>50</sub> (mg/L) <sup>b</sup>
1	25.4 ± 2.3	254.5 ± 5.6	22.1 ± 1.1	336.3 ± 4.2
2	62.7 ± 4.3	21.0 ± 3.6	68.1 ± 3.3	17.1 ± 3.1
3	32.5 ± 5.5	194.0 ± 4.5	31.9 ± 4.3	163.3 ± 5.1
4	39.7 ± 1.6	97.6 ± 3.1	38.6 ± 1.8	107.6 ± 2.5
5	56.9 ± 5.6	31.8 ± 3.3	51.7 ± 1.2	39.3 ± 3.6
6	48.9 ± 5.6	51.8 ± 6.5	47.6 ± 1.7	58.3 ± 5.1
7	53.7 ± 3.7	38.1 ± 2.1	50.6 ± 3.0	41.6 ± 3.2
8	45.2 ± 2.3	62.7 ± 1.3	48.5 ± 0.8	52.1 ± 1.8
9	37.9 ± 1.2	163.6 ± 3.2	27.2 ± 1.7	237.8 ± 2.9
10	41.7 ± 3.9	143.4 ± 5.1	31.2 ± 3.7	119.3 ± 4.7
11	26.1 ± 3.3	210.7 ± 3.9	29.7 ± 1.7	294.2 ± 4.3
12	41.1 ± 5.0	78.4 ± 3.1	48.3 ± 2.4	54.9 ± 3.6
13	31.1 ± 2.7	169.4 ± 4.2	28.4 ± 1.2	186.2 ± 4.7
14	35.9 ± 5.0	155.6 ± 5.1	26.7 ± 3.6	276.2 ± 3.9
15	38.4 ± 0.9	97.8 ± 2.5	44.8 ± 1.5	85.8 ± 2.1
16	33.0 ± 2.6	94.6 ± 1.3	32.7 ± 1.2	97.1 ± 1.8
17	58.4 ± 3.1	37.7 ± 1.8	53.8 ± 0.9	49.2 ± 1.2
18	35.5 ± 1.9	117.6 ± 3.2	39.1 ± 4.8	93.4 ± 3.0
19	35.2 ± 2.2	118.2 ± 2.5	47.8 ± 1.1	72.7 ± 2.8
20	38.6 ± 1.7	94.9 ± 2.8	49.4 ± 1.3	63.8 ± 2.5
21	31.3 ± 3.5	116.7 ± 3.1	46.9 ± 3.2	67.8 ± 3.6
22	23.2 ± 3.5	210.1 ± 2.8	35.5 ± 1.5	177.9 ± 3.1
23	49.9 ± 2.6	65.3 ± 1.0	51.0 ± 3.1	61.8 ± 1.5
24	63.5 ± 3.8	25.8 ± 1.3	61.8 ± 2.4	31.5 ± 2.1
25	53.7 ± 1.0	46.3 ± 1.8	52.5 ± 4.3	49.1 ± 1.2
26	39.6 ± 1.1	85.3 ± 3.7	41.5 ± 1.2	75.9 ± 3.3
27	46.9 ± 2.1	63.2 ± 4.1	47.2 ± 1.7	78.7 ± 3.8
28	50.5 ± 5.5	43.5 ± 2.1	52.3 ± 0.9	46.9 ± 1.7
29	48.6 ± 4.9	61.1 ± 2.6	46.5 ± 4.5	77.6 ± 2.8
30 <sup>c</sup>	100	1.8 ± 0.7	99.5 ± 0.2	2.1 ± 0.6
Thiodiazole copper	32.1 ± 4.3	92.5 ± 2.5	31.5 ± 4.9	99.6 ± 2.1

<sup>a</sup>All results are expressed as mean ± SD. <sup>b</sup>Experiments were repeated three times. <sup>c</sup>Compound 30 was designed based on the CoMFA model.

and *Xoc*. Among them, compounds 2, 5, 6, 7, 17, 24, 25, and 28 exhibited good inhibition activities against *Xoo*, with EC<sub>50</sub> values of 21.0, 31.8, 51.8, 38.1, 37.7, 25.8, 46.3, and 43.5 mg/L, respectively, which were superior to that of thiodiazole copper (92.5 mg/L). Compounds 2, 5, 7, 17, 24, 25, and 28 also showed good inhibition activities against *Xoc*, with EC<sub>50</sub> values

of 17.1, 39.3, 41.6, 49.2, 31.5, 49.1, and 46.9 mg/L, respectively, which were superior to that of thiodiazole copper (99.6 mg/L).

**3D-QSAR Analysis.** The CoMFA model was constructed according to the EC<sub>50</sub> values of compounds 1–29 against *Xoc*. The *q*<sup>2</sup>, *r*<sup>2</sup>, and *r*<sup>2</sup><sub>pred</sub> values were 0.6294, 0.9889, and 0.7078, respectively. Experimental values (pEC<sub>50</sub>), predicted values (pEC<sub>50</sub>), and residuals of training and test sets are listed in Table S1. The pEC<sub>50</sub> values of most compounds are concentrated near the trend line (Figure 5A), indicating that the CoMFA model might be reliable. In the steric field contour map (Figure 5B), a large yellow block is present around the 2-position of 1,3,4-thiadiazole, indicating that the introduction of a large group at the 2-position was not favorable for the antibacterial activity of compounds against *Xoc*, such as, 24 (R<sub>3</sub> = CH<sub>3</sub>, 31.5 mg/L) > 27 (R<sub>3</sub> = CH<sub>2</sub>CH<sub>2</sub>CF<sub>3</sub>, 78.7 mg/L). A few green blocks around the 5-position of 1,3,4-thiadiazole indicated that the introduction of a large group at the 5-position was favorable for the antibacterial activity of compounds against *Xoc*, such as, 2 (R<sub>1</sub> = CH(N=OCH<sub>3</sub>)Ph(2-CH<sub>3</sub>), 17.1 mg/L) > 4 (R<sub>1</sub> = Ph(2-OCH<sub>3</sub>), 107.6 mg/L). In the electrostatic field (Figure 5B), a large blue block around the 2-position indicated that the electronegative groups introduced at the 2-position were favorable for the antibacterial activities of compounds, such as, 5 (R<sub>2</sub> = 2-CF<sub>3</sub>-Ph, 39.3 mg/L) > 8 (R<sub>2</sub> = 4-CH<sub>3</sub>-Ph, 52.1 mg/L). In addition, when R<sub>3</sub> was the same substituent, the antibacterial activities of the sulfone compounds were higher than those of the sulfide compounds, such as, 24 (31.5 mg/L) > 9 (237.8 mg/L), and 23 (61.8 mg/L) > 10 (119.3 mg/L). The introduction of a large group at the 5-position of 1,3,4-thiadiazole and the introduction of a small negative group containing a sulfone group at the 2-position (Figure 5C) can improve the antibacterial activity of the compounds. According to the analysis results of the CoMFA model, compound 30, which had a good predictive value (pEC<sub>50</sub> = 5.168) was designed and synthesized. Compound 30 exhibited excellent antibacterial activity *in vitro* against *Xoc*, with an EC<sub>50</sub> value of 2.1 mg/L and an experimental pEC<sub>50</sub> value of 5.283. The experimental value of compound 30 was close to the predicted value, with a residual of 0.115, which indicates that the model has good prediction ability. In addition, compound 30 also has excellent antibacterial activity *in vitro* against *Xoo*, and its EC<sub>50</sub> value is 1.8 mg/L.

**Antibacterial Activities *In Vivo*.** Compound 30 exhibited moderate antibacterial activities against BLB and BLS at the concentration of 200 mg/L. As shown in Table 2 and Figure 6, the curative and protective activities of compound 30 against BLB were 46.1 and 51.3%, respectively, which were superior to those of thiodiazole copper (38.5 and 37.8%). Additionally, as shown in Figure 7 and Table 3, the *in vivo* protective and curative activities of compound 30 against BLS were 45.9 and 40.5%, respectively, which were better than those of thiodiazole copper (36.2 and 31.1%).

**Morphological Change.** The morphological change results of pathogens are illustrated in Figure 8. The cell morphology of the negative control was full and undamaged. Compared with the negative control, the *Xoo* and *Xoc* cell surfaces began to rupture after compound 30 treatment at a concentration of 5 mg/L. Furthermore, as the concentration of the compound increases, cell surface deformation and wrinkles gradually increase. Therefore, compound 30 may produce antibacterial activity *in vitro* by affecting the morphology of cells.

**Defensive Enzyme Activity.** The defensive enzyme activities of rice in the 30 + *Xoc*, CK + *Xoc*, and CK treatment groups were analyzed. The POD activity of the treatment group

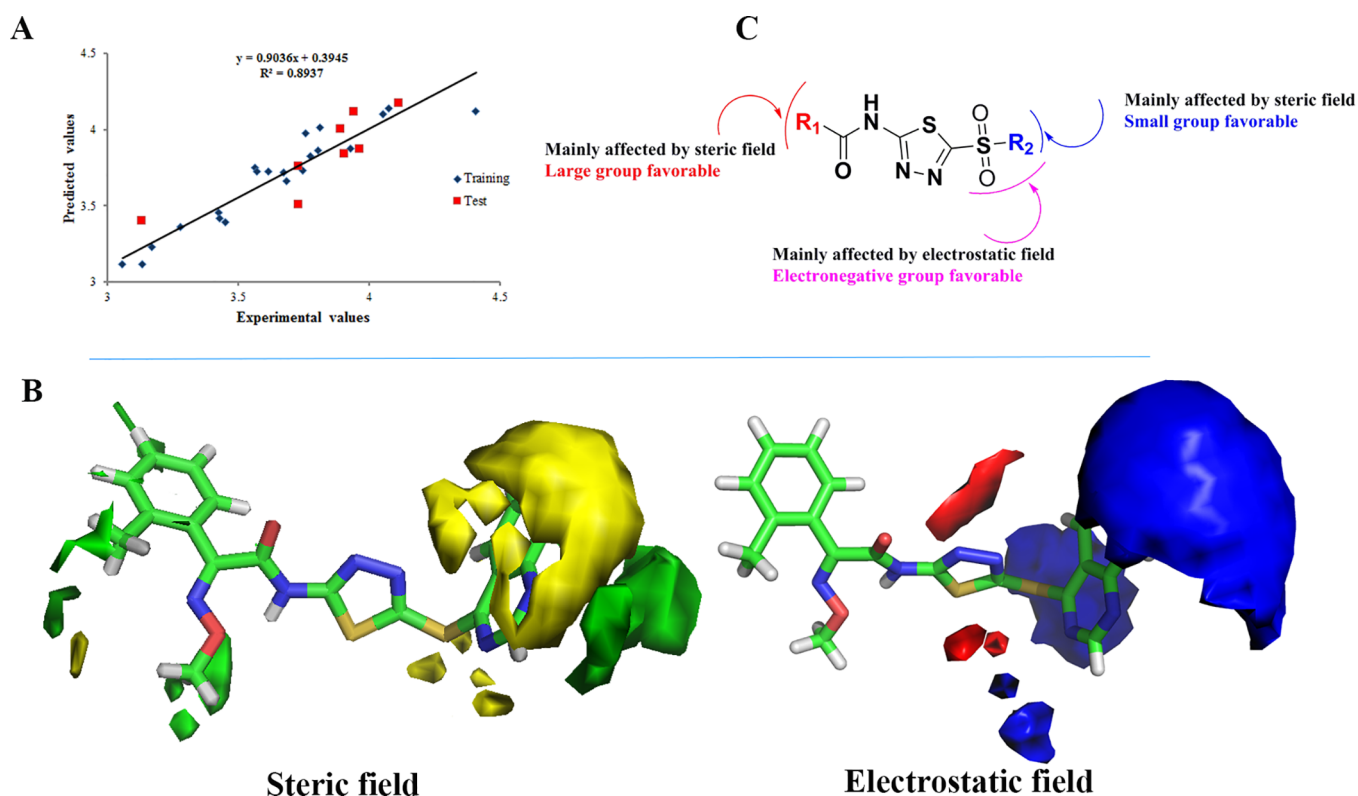


**Figure 5.** Result of the CoMFA analysis. Plots of experimental and predicted  $pEC_{50}$  values for the CoMFA model (A). The field contour maps of the CoMFA model based on the antibacterial activities against *Xoc* (B). Structure–activity relationships summarized based on the CoMFA model (C).

**Table 2. Protection and Curative Activities of Compound 30 against Rice Bacterial Leaf Blight under Greenhouse Conditions at 200 mg/L<sup>a</sup>**

treatments	morbidity (%)	disease index <sup>b</sup>	protective activity (%) <sup>c</sup>	disease index <sup>b</sup>	curative activity (%) <sup>c</sup>
30	100	40.0	51.3 ± 1.2a	46.7	46.1 ± 3.0a
thiodiazole copper	100	51.1	37.8 ± 2.9b	53.3	38.5 ± 1.5b
negative control	100	82.2		86.7	

<sup>a</sup>All results are expressed as mean ± SD. <sup>b</sup>Disease index, which is a comprehensive indicator of the overall incidence and severity. <sup>c</sup>Statistical analysis was performed by analysis of variance (ANOVA) in the SPSS 17.0 software with equal variances assumed ( $P > 0.05$ ). The different lowercase letters indicate curative activity with different treatment groups at  $P < 0.05$ .

30 + *Xoc* demonstrated an upward trend after *Xoc* infection, reaching its peak at 3 days (Figure 9A), which was 1.8- and 1.9-fold as much as that of CK + *Xoc* and CK treatment groups, respectively. The highest SOD activity of the treatment group 30 + *Xoc* at 1 day (Figure 9B) was 1.0- and 1.5-fold of CK + *Xoc* and CK treatment groups, respectively. Compared with other treatment groups, the CAT activity of the 30 + *Xoc* treatment group began to increase at 5 days (Figure 9C) and reached its peak at 7 days, which was 2.1- and 1.3-fold as much as those of the CK + *Xoc* and CK treatment groups, respectively. The PAL activity of the compound 30 treatment group demonstrated no obvious upward trend compared with that of other treatment groups (Figure 9D). Compound 30 may enhance related enzymes' (POD, CAT, and SOD) activities to increase the resistance of rice to disease.

**Analysis of DEPs.** The iBAQ algorithm of the protein profile label-free technology was used to quantify the total protein of rice leaves of the 30 + *Xoc* and CK + *Xoc* treatment groups. The 1527 proteins of the 30 + *Xoc* and CK + *Xoc* treatment groups were identified. As shown in Figure S1, a total of 1285 and 1155 proteins were identified in the 30 + *Xoc* and CK + *Xoc* treatment groups, respectively. In addition, 371 and 241 proteins were differentially expressed in the 30 + *Xoc* and CK + *Xoc* treatment groups, respectively. Of the total number of identified DEPs, 168 upregulated (red dots) and 58 downregulated (blue dots) in 30 + *Xoc* and CK + *Xoc* treatment groups (Figure S2).

**GO Functional Classification.** The annotations of DEPs were analyzed using the differential annotation database, the visualization database, and Integrated Discovery 6.8. The differentially expressed proteins identified in the cellular components, molecular functions, and biological processes were analyzed for GO term enrichment ( $p < 0.05$ ). As shown in Figure 10, the main cellular components were integral components of the membrane, nucleus, chloroplast stroma, chloroplast, apoplast, chloroplast envelope, extracellular region, chloroplast thylakoid membrane, cytosol, ribosome, cytoplasm, and mitochondrion. Most of DEPs were significantly enriched in molecular functions, including the following: structural constituent of ribosome, peroxidase activity, oxidoreductase activity, DNA binding, RNA binding, nucleic acid binding, zinc ion binding, electron carrier activity, ATP binding, GTP binding, calcium ion binding, hydrolase activity, nucleotide binding, and heme binding. The identified biological processes included the carbohydrate metabolic process, photosynthesis, chlorophyll biosynthetic process, pentose-phosphate shunt, carotenoid biosynthetic process, thylakoid membrane organization, isopentenyl diphosphate biosynthetic process, protein

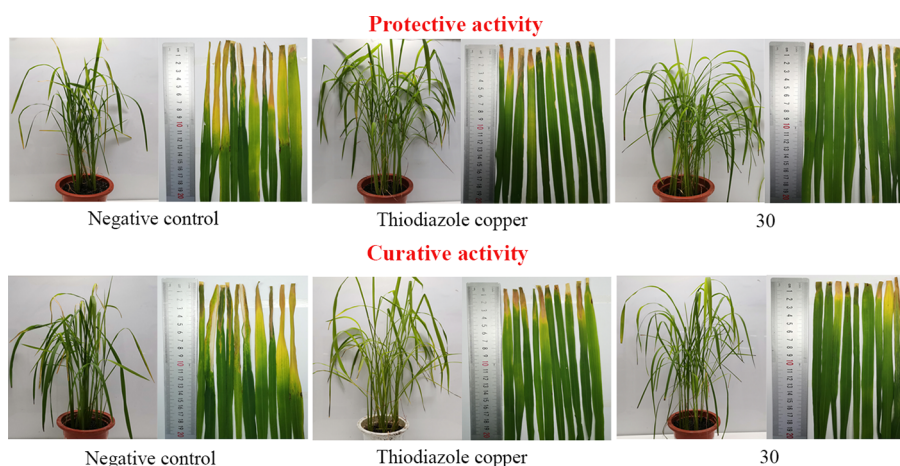


**Figure 6.** Protective and curative activities of compound 30 against rice bacterial leaf blight at 200 mg/L.

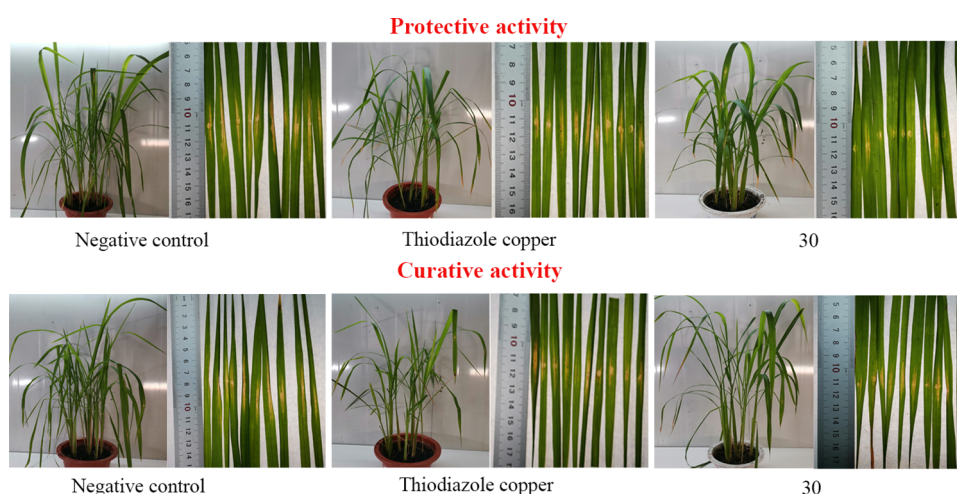


**Figure 7.** Protective and curative activities of compound 30 against rice bacterial leaf streak at 200 mg/L.

**Table 3. Protection and Curative Activities of Compound 30 against Rice Bacterial Leaf Streak under Greenhouse Conditions at 200 mg/L<sup>a</sup>**

treatments	average lesion length (cm)	protective activity (%) <sup>b</sup>	average lesion length (cm)	curative activity (%) <sup>b</sup>
30	2.6	45.9 ± 3.5a	2.7	40.5 ± 2.6a
thiodiazole copper	3.0	36.2 ± 1.1b	3.1	31.1 ± 1.8b
negative control	4.7		4.5	

<sup>a</sup>All results are expressed as mean ± SD. <sup>b</sup>Statistical analysis was performed by analysis of variance (ANOVA) in the SPSS 17.0 software with equal variances assumed ( $P > 0.05$ ). The different lowercase letters indicate curative activity with different treatment groups at  $P < 0.05$ .

folding, photosystem II assembly, hydrogen peroxide catabolic process, glycolytic process, translation, rRNA processing, response to oxidative stress, and cell redox homeostasis.

**KEGG Classification.** The possible biological pathways of the 30 + *Xoc* and CK + *Xoc* treatment groups were identified through KEGG analysis. As shown in Figure S3 and Table 4, 19 proteins were mainly enriched in the glycolysis/gluconeogenesis pathway. There were 4 upregulated proteins, 2 downregulated proteins, and 13 proteins with no difference. The glycolysis/

gluconeogenesis pathway is the main pathway whereby rice obtains energy after infection with pathogenic bacteria.<sup>42</sup> Among the DEPs enriched in the glycolysis/gluconeogenesis pathway, fructose-1,6-bisphosphatase (F16P2\_ORYSJ), aldehyde dehydrogenase ALDH2b (Q9FRX7\_ORYSJ), dihydroli-poyl dehydrogenase (Q9ASP4\_ORYSJ), and the dihydroli-poa-mide acetyltransferase component of pyruvate dehydrogenase complex (Q6ZKB1\_ORYSJ) were upregulated. In contrast, glucose-6-phosphate 1-epimerase (Q6K2P3\_ORYSJ) and fructose-bisphosphate aldolase (Q94JJ0\_ORYSJ) were down-regulated. In the process of plant photosynthesis, triose phosphate exported from the chloroplast to the cytoplasm was converted to sucrose by fructose-1,6-bisphosphatase in the cytoplasm.<sup>43</sup> Compound 30 might promote photosynthesis by upregulating fructose-1,6-bisphosphatase. Pathogenic bacterial infections often increase the content of reactive oxygen species (ROS) in plants. ROS induce lipid peroxidation and damage to proteins and DNA, and produce many harmful substances, such as aldehydes.<sup>44,45</sup> The production of related enzymes may remove harmful aldehydes, such as the aldehyde dehydrogenase ALDH2b, which has NAD<sup>+</sup>-linked activity and can oxidize acetaldehyde, glycolaldehyde, and propionaldehyde in plants.<sup>46</sup> After compound 30 treatment, the contents of SOD, POD, and CAT increased, which may help reduce the accumulation of harmful aldehyde substances caused by ROS in plants.

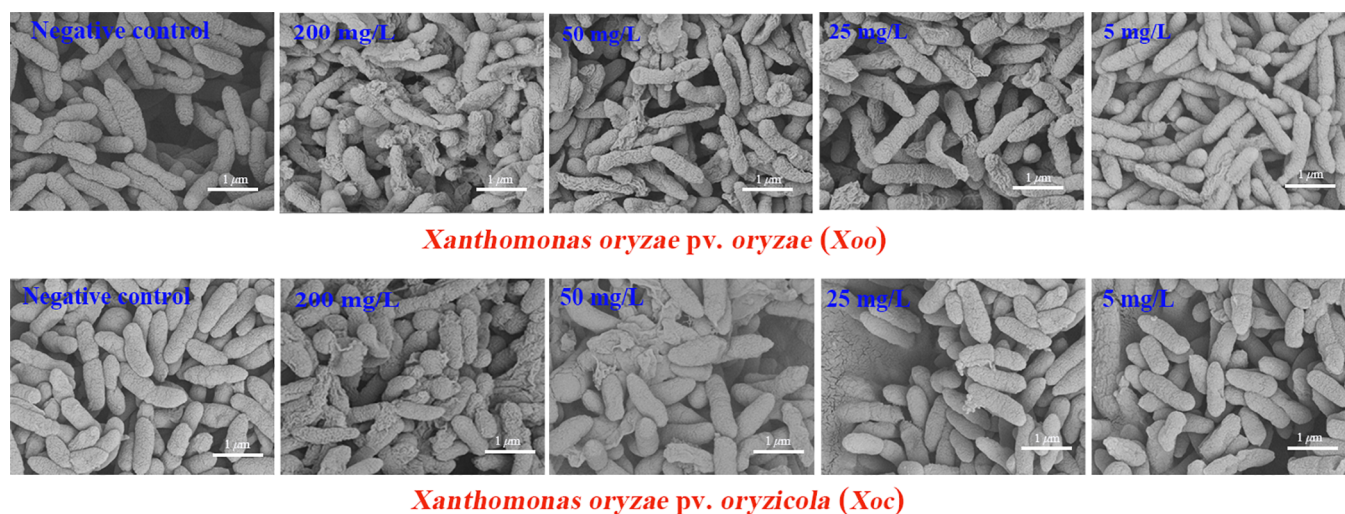


**Figure 8.** The effects of compound **30** at different concentrations on the morphology of Xoo and Xoc cells.

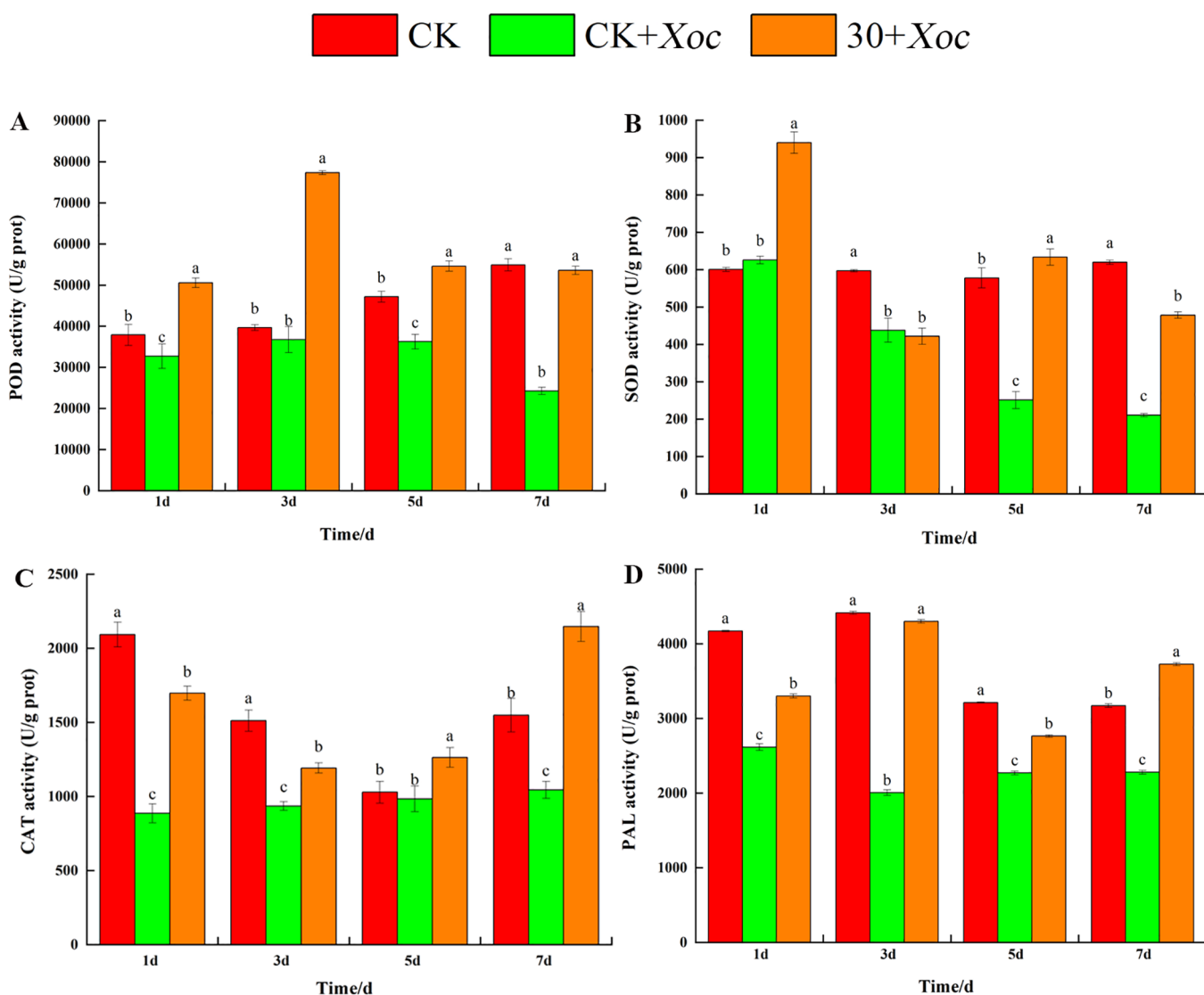


**Figure 9.** Effects of compound **30** on POD (A), SOD (B), CAT (C), and PAL (D) activities in the rice leaves. Values are the means and standard deviations of three independent experiments. Different lowercase letters indicate values with significant differences among different treatment groups, according to one-way ANOVA ( $P < 0.05$ ).

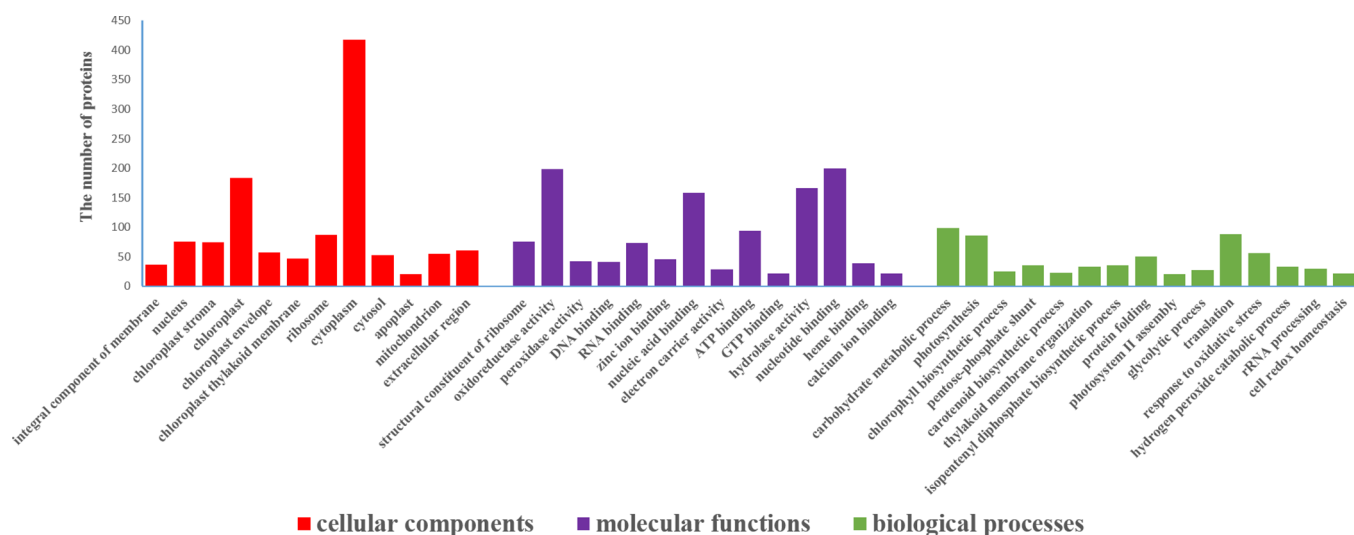


**Figure 10.** Cellular components, molecular functions, and biological processes involving DEPs in the 30 + *Xoc* and CK + *Xoc* treatment groups.

**Table 4.** Differentially Expressed Proteins Involved in Glycolysis/Gluconeogenesis Pathway

ID	protein names	gene names	organism	regulate <sup>a</sup>
F16P2_ORYSJ	fructose-1,6-bisphosphatase (EC 3.1.3.11)	Os01g0866400	<i>Oryza sativa</i> subsp. <i>japonica</i> (rice)	1
F16P1_ORYSJ	fructose-1,6-bisphosphatase, chloroplastic (FBPase) (EC 3.1.3.11)	Os03g0267300	<i>Oryza sativa</i> subsp. <i>japonica</i> (rice)	0
G3PC2_ORYSJ	glyceraldehyde-3-phosphate dehydrogenase 2, cytosolic (EC 1.2.1.12)	Os04g0486600	<i>Oryza sativa</i> subsp. <i>japonica</i> (rice)	0
Q9FRX7_ORYSJ	aldehyde dehydrogenase ALDH2b	Os06g0270900	<i>Oryza sativa</i> subsp. <i>japonica</i> (rice)	1
Q6YPG2_ORYSJ	acetyltransferase component of pyruvate dehydrogenase complex (EC 2.3.1.12)	Os02g0105200	<i>Oryza sativa</i> subsp. <i>japonica</i> (rice)	0
Q9ASP4_ORYSJ	dihydrolipoyl dehydrogenase (EC 1.8.1.4)	Os01g0328700	<i>Oryza sativa</i> subsp. <i>japonica</i> (rice)	1
Q69K00_ORYSJ	Os09g0535000 protein	Os09g0535000	<i>Oryza sativa</i> subsp. <i>japonica</i> (rice)	0
Q7XKB5_ORYSJ	pyruvate kinase (EC 2.7.1.40)	Os04g0677500	<i>Oryza sativa</i> subsp. <i>japonica</i> (rice)	0
Q69V57_ORYSJ	fructose-bisphosphate aldolase (EC 4.1.2.13)	Os06g0608700	<i>Oryza sativa</i> subsp. <i>japonica</i> (rice)	0
Q53PY7_ORYSJ	Os11g0150100 protein	Os11g0150100	<i>Oryza sativa</i> subsp. <i>japonica</i> (rice)	0
Q6K2P3_ORYSJ	glucose-6-phosphate 1-epimerase (EC 5.1.3.15)	Os09g0327400	<i>Oryza sativa</i> subsp. <i>japonica</i> (rice)	-1
Q94JJ0_ORYSJ	fructose-bisphosphate aldolase (EC 4.1.2.13)	Os01g0118000	<i>Oryza sativa</i> subsp. <i>japonica</i> (rice)	-1
Q6H6C7_ORYSJ	phosphoglycerate kinase (EC 2.7.2.3)	Os02g0169300	<i>Oryza sativa</i> subsp. <i>japonica</i> (rice)	0
Q10P35_ORYSJ	phosphopyruvate hydratase (EC 4.2.1.11)	Os03g0248600	<i>Oryza sativa</i> subsp. <i>japonica</i> (rice)	0
Q5VNT9_ORYSJ	phosphopyruvate hydratase (EC 4.2.1.11)	Os06g0136600	<i>Oryza sativa</i> subsp. <i>japonica</i> (rice)	0
Q654L9_ORYSJ	acetyltransferase component of pyruvate dehydrogenase complex (EC 2.3.1.12)	Os06g0499900	<i>Oryza sativa</i> subsp. <i>japonica</i> (rice)	0
Q6ZKB1_ORYSJ	dihydrolipoamide acetyltransferase component of pyruvate dehydrogenase complex (EC 2.3.1.-)	Os08g0431300	<i>Oryza sativa</i> subsp. <i>japonica</i> (rice)	1
Q6Z9G0_ORYSJ	Os08g0440800 protein	Os08g0440800	<i>Oryza sativa</i> subsp. <i>japonica</i> (rice)	0
Q2QWU7_ORYSJ	dihydrolipoamide acetyltransferase component of pyruvate dehydrogenase complex (EC 2.3.1.-)	Os12g0182200	<i>Oryza sativa</i> subsp. <i>japonica</i> (rice)	0

<sup>a</sup>1, upregulated protein expression; 0, protein expression did not change; -1, downregulated protein expression.

Dihydrolipoyl dehydrogenase is a tricarboxylic acid cycle-related protein that is an NAD<sup>+</sup>-dependent oxidoreductase that catalyzes the oxidation of dihydroacyl moieties.<sup>47</sup> The dihydrolipoamide acetyltransferase component of the pyruvate dehydrogenase complex is a metabolic factor in the calorie

restriction pathway that improves metabolic fitness by regulating central metabolic enzymes.<sup>48</sup> The results revealed that treatment with compound **30** may activate the glycolysis/gluconeogenesis pathway, promote the specific expression of related proteins,

increase related enzymes activities, and improve the disease resistance of plants.

In summary, a series of novel 1,3,4-thiadiazole derivatives containing an amide moiety were designed and synthesized, and their antibacterial activities were evaluated. Compound **30**, which showed better antibacterial activity *in vitro* and *in vivo*, was designed and synthesized according to the CoMFA model. Compound **30** may exhibit antibacterial activity *in vitro* by changing cell morphology and inhibiting cell growth. In addition, compound **30** can increase the activity of related defense enzymes and upregulate DEP expression in the glycolysis/gluconeogenesis pathway to increase rice disease resistance. Therefore, 1,3,4-thiadiazole derivatives containing amide moieties can be used as leading structures for discovering new antibacterial agents.

## ■ ASSOCIATED CONTENT

### SI Supporting Information

The Supporting Information is available free of charge at <https://pubs.acs.org/doi/10.1021/acs.jafc.1c01626>.

The physical and chemical properties, and  $^1\text{H}$  NMR,  $^{13}\text{C}$  NMR, and HRMS of target compounds **1–30** were represented in Supporting Information I (PDF)

All identified proteins can be found in Supporting Information II (XLSX)

## ■ AUTHOR INFORMATION

### Corresponding Authors

**Deyu Hu** — State Key Laboratory Breeding Base of Green Pesticide and Agricultural Bioengineering, Key Laboratory of Green Pesticide and Agricultural Bioengineering, Ministry of Education, Guizhou University, Guiyang 550025, P.R. China; [orcid.org/0000-0001-7843-371X](https://orcid.org/0000-0001-7843-371X); Phone: + 86-851083620521; Email: [dyhu@gzu.edu.cn](mailto:dyhu@gzu.edu.cn); Fax: + 86-0851-83622211

**Baoan Song** — State Key Laboratory Breeding Base of Green Pesticide and Agricultural Bioengineering, Key Laboratory of Green Pesticide and Agricultural Bioengineering, Ministry of Education, Guizhou University, Guiyang 550025, P.R. China; [orcid.org/0000-0002-4237-6167](https://orcid.org/0000-0002-4237-6167); Email: [basong@gzu.edu.cn](mailto:basong@gzu.edu.cn)

### Authors

**Zhibing Wu** — State Key Laboratory Breeding Base of Green Pesticide and Agricultural Bioengineering, Key Laboratory of Green Pesticide and Agricultural Bioengineering, Ministry of Education, Guizhou University, Guiyang 550025, P.R. China

**Jin Shi** — State Key Laboratory Breeding Base of Green Pesticide and Agricultural Bioengineering, Key Laboratory of Green Pesticide and Agricultural Bioengineering, Ministry of Education, Guizhou University, Guiyang 550025, P.R. China

**Jixiang Chen** — State Key Laboratory Breeding Base of Green Pesticide and Agricultural Bioengineering, Key Laboratory of Green Pesticide and Agricultural Bioengineering, Ministry of Education, Guizhou University, Guiyang 550025, P.R. China

Complete contact information is available at: <https://pubs.acs.org/doi/10.1021/acs.jafc.1c01626>

### Notes

The authors declare no competing financial interest.

## ■ ACKNOWLEDGMENTS

Thanks to the National Key Research and Development Program (2018YFD0200100) and the National Natural Science Foundation of China (21672044) for supporting the project.

## ■ ABBREVIATIONS

Xoc, *Xanthomonas oryzae* pv. *oryzicola*; Xoo, *Xanthomonas oryzae* pv. *oryzae*; BLB, rice bacterial leaf blight; BLS, rice bacterial leaf streak;  $\text{EC}_{50}$ , half-maximal effective concentration; TC, thiadiazole copper; DCM, dichloromethane; DMF, *N,N*-dimethylformamide; 3D-QSAR, three-dimensional quantitative structure–activity relationship; CoMFA, comparative molecular field analysis;  $q^2$ , cross-validation coefficient;  $r^2$ , non-cross-validation coefficient;  $r^2_{\text{pred}}$ , non-cross-validation coefficient of the prediction; PBS, phosphate-buffered saline; SOD, superoxide dismutase; POD, peroxidase; PAL, phenylalanine ammonia lyase; CAT, catalase; DEPs, differentially expressed proteins; DTT, dithiothreitol; iBAQ, intensity-based absolute quantification; GO, Gene Ontology; KEGG, Kyoto Encyclopedia of Genes and Genomes; ROS, reactive oxygen species.

## ■ REFERENCES

- Jiang, N.; Yan, J.; Liang, Y. L.; He, Z. Z.; Wu, Y. T.; Zeng, Q.; Liu, X. J.; Peng, J. H. Resistance genes and their interactions with bacterial blight/leaf streak pathogens (*Xanthomonas oryzae*) in rice (*Oryza sativa* L.)—an updated review. *Rice* **2020**, *13*, 1–12.
- Li, D. X.; Wang, L. J.; Teng, S. L.; Zhang, G. G.; Guo, L. J.; Mao, Q.; Wang, W.; Li, M. M.; Chen, L. Proteomics analysis of rice proteins up-regulated in response to bacterial leaf streak disease. *J. Plant Biol.* **2012**, *55*, 316–324.
- Srinivasan, B.; Gnanamanickam, S. S. Identification of a new source of resistance in wild rice, *oryza rufipogon* to bacterial blight of rice caused by indian strains of *Xanthomonas oryzae* pv. *oryzae*. *Curr. Sci.* **2005**, *88*, 1229–1231.
- Triplett, L. R.; Cohen, S. P.; Heffelfinger, C.; Schmidt, C. L.; Huerta, A.; Tekete, C.; Verdier, V.; Bogdanove, A. J.; Leach, J. E. A resistance locus in the American heirloom rice variety Carolina gold select is triggered by TAL effectors with diverse predicted targets and is effective against African strains of *Xanthomonas oryzae* pv. *oryzicola*. *Plant J.* **2016**, *87*, 472–483.
- Tang, D.; Wu, W.; Li, W.; Lu, H.; Worland, A. J. Mapping of QTLs conferring resistance to bacterial leaf streak in rice. *Theor. Appl. Genet.* **2000**, *101*, 286–291.
- Zhang, J. H.; Wei, C. L.; Li, S. Y.; Hu, D. Y.; Song, B. A. Discovery of novel bis-sulfoxide derivatives bearing acylhydrazone and benzothiazole moieties as potential antibacterial agents. *Pestic. Biochem. Physiol.* **2020**, *167*, 104605.
- Lin, Y.; He, Z.; Roskopf, E. N.; Conn, K. L.; Powell, C. A.; Lazarovits, G. A nylon membrane bag assay for determination of the effect of chemicals on soilborne plant pathogens in soil. *Plant Dis.* **2010**, *94*, 201–206.
- Li, P.; Shi, L.; Yang, X.; Yang, L.; Chen, X. W.; Wu, F.; Shi, Q. C.; Xu, W. M.; He, M.; Hu, D. Y.; Song, B. A. Design, synthesis, and antibacterial activity against rice bacterial leaf blight and leaf streak of 2,5-substituted-1,3,4-oxadiazole/thiadiazole sulfone derivative. *Bioorg. Med. Chem. Lett.* **2014**, *24*, 1677–1680.
- Chen, J. X.; Yi, C.; Wang, S. B.; Wu, S. K.; Li, S. Y.; Hu, D. Y.; Song, B. A. Novel amide derivatives containing 1,3,4-thiadiazole moiety: Design, synthesis, nematocidal and antibacterial activities. *Bioorg. Med. Chem. Lett.* **2019**, *29*, 1203–1210.
- Hu, Y.; Li, C. Y.; Wang, X. M.; Yang, Y. H.; Zhu, H. L. 1,3,4-thiadiazole: Synthesis, reactions, and applications in medicinal, agricultural, and materials chemistry. *Chem. Rev.* **2014**, *45*, 5572–5610.
- Wu, Q.; Cai, H.; Yuan, T.; Li, S. Y.; Gan, X. H.; Song, B. A. Novel vanillin derivatives containing a 1,3,4-thiadiazole moiety as potential antibacterial agents. *Bioorg. Med. Chem. Lett.* **2020**, *30*, 127113.

- (12) Zhang, M.; Xu, W. M.; Wei, K.; Liu, H. W.; Yang, Q.; Liu, Q.; Yang, L. Y.; Luo, Y. Q.; Xue, W. Synthesis and evaluation of 1,3,4-thiadiazole derivatives containing cyclopentylpropionamide as potential antibacterial agent. *J. Heterocycl. Chem.* **2019**, *20*, 1966–1977.
- (13) Li, P.; Shi, L.; Gao, M. N.; Yang, X.; Xue, W.; Jin, L. H.; Hu, D. Y.; Song, B. A. Antibacterial activities against rice bacterial leaf blight and tomato bacterial wilt of 2-mercapto-5-substituted-1,3,4-oxadiazole/thiadiazole derivatives. *Bioorg. Med. Chem. Lett.* **2015**, *25*, 481–484.
- (14) Zine, H.; Rifai, L. A.; Faize, M.; Bentiss, F.; Guesmi, S.; Laachir, A.; Smaili, A.; Makroum, K.; Sahibed-Dine, A.; Koussa, T. Induced resistance in tomato plants against verticillium wilt by the binuclear nickel coordination complex of the ligand 2,5-bis(pyridin-2-yl)-1,3,4-thiadiazole. *J. Agric. Food Chem.* **2016**, *64*, 2661–2667.
- (15) Zou, X. J.; Lai, L. H.; Jin, G. Y.; Zhang, Z. X. Synthesis, fungicidal activity, and 3D-QSAR of pyridazinone-substituted 1,3,4-oxadiazoles and 1,3,4-thiadiazoles. *J. Agric. Food Chem.* **2002**, *50*, 3757–3760.
- (16) Lv, M.; Liu, G. C.; Jia, M. H.; Xu, H. Synthesis of matrinic amide derivatives containing 1,3,4-thiadiazole scaffold as insecticidal/acaricidal agents. *Bioorg. Chem.* **2018**, *81*, 88–92.
- (17) Dai, H.; Li, G.; Chen, J.; Shi, Y. J.; Ge, S. S.; Fan, C. G.; He, H. B. Synthesis and biological activities of novel 1,3,4-thiadiazole-containing pyrazole oxime derivatives. *Bioorg. Med. Chem. Lett.* **2016**, *26*, 3818–3821.
- (18) Gan, X. H.; Hu, D. Y.; Chen, Z.; Wang, Y. J.; Song, B. A. Synthesis and antiviral evaluation of novel 1,3,4-oxadiazole/thiadiazole-chalcone conjugates. *Bioorg. Med. Chem. Lett.* **2017**, *27*, 4298–4301.
- (19) Chen, Z.; Li, D.; Xu, N.; Fang, J.; Yu, Y.; Hou, W.; Ruan, H. Q.; Zhu, P. P.; Ma, R. C.; Lu, S. Y.; Cao, D. H.; Wu, R.; Ni, M. W.; Zhang, W.; Su, W. K.; Ruan, B. H. Novel 1,3,4-selenadiazole-containing kidney-type glutaminase inhibitors showed improved cellular uptake and antitumor activity. *J. Med. Chem.* **2019**, *62*, 589–603.
- (20) Xu, H.; Xu, M.; Sun, Z. Q.; Li, S. C. Preparation of matrinic/oxymatrinic amide derivatives as insecticidal/acaricidal agents and study on the mechanisms of action against tetranychus cinnabarinus. *J. Agric. Food Chem.* **2019**, *67*, 12182–12190.
- (21) Wang, B. L.; Zhu, H. W.; Ma, Y.; Xiong, L. X.; Li, Y. Q.; Zhao, Y.; Zhang, J. F.; Chen, Y. W.; Zhou, S.; Li, Z. M. Synthesis, insecticidal activities, and SAR studies of novel pyridylpyrazole acid derivatives based on amide bridge modification of anthranilic diamide insecticides. *J. Agric. Food Chem.* **2013**, *61*, 5483–5493.
- (22) Sun, R. F.; Wang, Z. W.; Li, Y. Q.; Xiong, L. X.; Liu, Y. X.; Wang, Q. M. Design, synthesis, and insecticidal evaluation of new benzoylureas containing amide and sulfonate groups based on the sulfonylurea receptor protein binding site for diflubenzuron and glibenclamide. *J. Agric. Food Chem.* **2013**, *61*, 517–522.
- (23) Luo, D. X.; Guo, S. X.; He, F.; Chen, S. H.; Dai, A. L.; Zhang, R. F.; Wu, J. Design, synthesis, and bioactivity of  $\alpha$ -ketoamide derivatives bearing a vanillin skeleton for crop diseases. *J. Agric. Food Chem.* **2020**, *68*, 7226–7234.
- (24) Xiang, J.; Liu, D. Y.; Chen, J. X.; Hu, D. Y.; Song, B. A. Design and synthesis of novel 1,3,4-oxadiazole sulfone compounds containing 3,4-dichloroisothiazolylamide moiety and evaluation of rice bacterial activity. *Pestic. Biochem. Physiol.* **2020**, *170*, 104695.
- (25) Zhou, X.; Feng, Y. M.; Qi, P. Y.; Shao, W. B.; Wu, Z. B.; Liu, L. W.; Wang, Y.; Ma, H. D.; Wang, P. Y.; Li, Z.; Yang, S. Synthesis and docking study of *N*-(cinnamoyl)-*N'*-(substituted)acryloyl hydrazide derivatives containing pyridinium moieties as a novel class of filamentous temperature-sensitive protein Z inhibitors against the intractable *Xanthomonas oryzae* pv. *oryzae* infections in rice. *J. Agric. Food Chem.* **2020**, *68*, 8132–8142.
- (26) Kalgutkar, A. S.; Marnett, A. B.; Crews, B. C.; Rimmel, R. P.; Marnett, L. J. Ester and amide derivatives of the nonsteroidal antiinflammatory drug, indomethacin, as selective cyclooxygenase-2 inhibitors. *J. Med. Chem.* **2000**, *43*, 2860–2870.
- (27) Hu, D. Y.; Wan, Q. Q.; Yang, S.; Song, B. A.; Bhadury, P. S.; Jin, L. H.; Yan, K.; Liu, F.; Chen, Z.; Xue, W. Synthesis and antiviral activities of amide derivatives containing the  $\gamma$ -aminophosphonate moiety. *J. Agric. Food Chem.* **2008**, *56*, 998–1001.
- (28) Lan, X. M.; Xie, D. D.; Yin, L. M.; Wang, Z. Z.; Chen, J.; Zhang, A. W.; Song, B. A.; Hu, D. Y. Novel  $\alpha,\beta$ -unsaturated amide derivatives bearing  $\alpha$ -amino phosphonate moiety as potential antiviral agents. *Bioorg. Med. Chem. Lett.* **2017**, *27*, 4270–4273.
- (29) Ghosh, S.; Liu, Y.; Garg, G.; Anyika, M.; McPherson, N. T.; Ma, J.; Dobrowsky, R. T.; Blagg, B. S. Diverging novobiocin anti-cancer activity from neuroprotective activity through modification of the amide tail. *ACS Med. Chem. Lett.* **2016**, *7*, 813–818.
- (30) Luo, H.; Liu, J. J.; Jin, L. H.; Hu, D. Y.; Chen, Z.; Yang, S.; Wu, J.; Song, B. A. Synthesis and antiviral bioactivity of novel (1*E*, 4*E*)-1-aryl-5-(2-(quinazolin-4-yloxy)phenyl)-1,4-pentadien-3-one derivatives. *Eur. J. Med. Chem.* **2013**, *63*, 662–669.
- (31) Kalimuthu, P.; John, S. A. Nanostructured electropolymerized film of 5-amino-2-mercapto-1,3,4-thiadiazole on glassy carbon electrode for the selective determination of l-cysteine. *Electrochem. Commun.* **2009**, *11*, 367–370.
- (32) Liu, H. W.; Ji, Q. T.; Ren, G. G.; Wang, F.; Su, F.; Wang, P. Y.; Zhou, X.; Wu, Z. B.; Li, Z.; Yang, S. Antibacterial functions and proposed modes of action of novel 1,2,3,4-tetrahydro- $\beta$ -carboline derivatives that possess an attractive 1,3-diaminopropan-2-ol pattern against rice bacterial blight, kiwifruit bacterial canker, and citrus bacterial canker. *J. Agric. Food Chem.* **2020**, *68*, 12558–12568.
- (33) Li, P.; Hu, D. Y.; Xie, D. D.; Chen, J. X.; Jin, L. H.; Song, B. A. Design, synthesis, and evaluation of new sulfone derivatives containing a 1,3,4-oxadiazole moiety as active antibacterial agents. *J. Agric. Food Chem.* **2018**, *66*, 3093–3100.
- (34) Wang, Y. L.; Wang, F.; Shi, X. X.; Jia, C. Y.; Wu, F. X.; Hao, G. F.; Yang, G. F. Cloud 3D-QSAR: A web tool for the development of quantitative structure–activity relationship models in drug discovery. *Briefings Bioinf.* **2020**.
- (35) Shi, L.; Li, P.; Wang, W.; Gao, M. N.; Wu, Z. X.; Song, X. P.; Hu, D. Y. Antibacterial activity and mechanism of action of sulfone derivatives containing 1,3,4-oxadiazole moieties on rice bacterial leaf blight. *Molecules* **2015**, *20*, 11660–11675.
- (36) Chen, J. X.; Luo, Y. Q.; Wei, C. Q.; Wu, S. K.; Wu, R.; Wang, S. B.; Hu, D. Y.; Song, B. A. Novel sulfone derivatives containing a 1,3,4-oxadiazole moiety: Design and synthesis based on the 3D-QSAR model as potential antibacterial agent. *Pest Manage. Sci.* **2020**, *76*, 3188–3198.
- (37) Zou, H. S.; Yuan, L.; Guo, W.; Li, Y. R.; Che, Y. Z.; Zou, L. F.; Chen, G. Y. Construction of a Tn5-tagged mutant library of *Xanthomonas oryzae* pv. *oryzicola* as an invaluable resource for functional genomics. *Curr. Microbiol.* **2011**, *62*, 908–916.
- (38) Jiang, S. C.; Su, S. J.; Chen, M.; Peng, F.; Zhou, Q.; Liu, T. T.; Liu, L. W.; Xue, W. Antibacterial activities of novel dithiocarbamate-containing 4H-chromen-4-one derivatives. *J. Agric. Food Chem.* **2020**, *68*, 5641–5647.
- (39) Long, Q. S.; Liu, L. W.; Zhao, Y. L.; Wang, P. Y.; Chen, B.; Li, Z.; Yang, S. Fabrication of furan-functionalized quinazoline hybrids: Their antibacterial evaluation, quantitative proteomics, and induced phytopathogen morphological variation studies. *J. Agric. Food Chem.* **2019**, *67*, 11005–11017.
- (40) Yu, L.; Wang, W. L.; Zeng, S.; Chen, Z.; Yang, A. M.; Shi, J.; Zhao, X. Z.; Song, B. A. Label-free quantitative proteomics analysis of cytosinepeptidomycin responses in southern rice black-streaked dwarf virus-infected rice. *Pestic. Biochem. Physiol.* **2018**, *147*, 20–26.
- (41) Yang, A. M.; Yu, L.; Chen, Z.; Zhang, S. X.; Shi, J.; Zhao, X. Z.; Yang, Y. Y.; Hu, D. Y.; Song, B. A. Label-free quantitative proteomic analysis of chitosan oligosaccharide-treated rice infected with southern rice black-streaked dwarf virus. *Viruses* **2017**, *9*, 115–131.
- (42) Bailey-Serres, J.; Fukao, T.; Gibbs, D. J.; Holdsworth, M. J.; Lee, S. C.; Licausi, F.; Perata, P.; Voesenek, L. A.; van Dongen, J. T. Making sense of low oxygen sensing. *Trends Plant Sci.* **2012**, *17*, 129–138.
- (43) Du, S.; Guan, Z.; Hao, L.; Song, Y.; Shao, S. Fructose-bisphosphate aldolase is a potential metastasis-associated marker of lung squamous cell carcinoma and promotes lung cell tumorigenesis and migration. *PLoS One* **2014**, *9*, No. e85804.
- (44) Guo, X. L.; Wang, Y. Y.; Lu, H. J.; Cai, X. Y.; Wang, X. X.; Zhou, Z. L.; Wang, C. Y.; Wang, Y. H.; Zhang, Z. M.; Wang, K. B.; Liu, F. Genome-wide characterization and expression analysis of the aldehyde

dehydrogenase (*ALDH*) gene superfamily under abiotic stresses in cotton. *Gene* **2017**, *628*, 230–245.

(45) Gill, S. S.; Tuteja, N. Reactive oxygen species and antioxidant machinery in abiotic stress tolerance in crop plants. *Plant Physiol. Biochem.* **2010**, *48*, 909–930.

(46) Tsuji, H.; Tsutsumi, N.; Sasaki, T.; Hirai, A.; Nakazono, M. Organ-specific expressions and chromosomal locations of two mitochondrial aldehyde dehydrogenase genes from rice (*Oryza sativa* L.), *ALDH2a* and *ALDH2b*. *Gene* **2003**, *305*, 195–204.

(47) Yan, L. J.; Sumien, N.; Thangthaeng, N.; Forster, M. J. Reversible inactivation of dihydrolipoamide dehydrogenase by mitochondrial hydrogen peroxide. *Free Radical Res.* **2013**, *47*, 123–133.

(48) Easlson, E.; Tsang, F.; Dilova, L.; Wang, C.; Lu, S. P.; Skinner, C.; Lin, S. J. The dihydrolipoamide acetyltransferase is a novel metabolic longevity factor and is required for calorie restriction-mediated life span extension. *J. Biol. Chem.* **2007**, *282*, 6161–6171.